Journal of proteome research

Article

pubs.acs.org/jpr

Loss of Correlations among Proteins in Brains of the Ts65Dn Mouse Model of Down Syndrome

Md. Mahiuddin Ahmed,[†] Xiaolu Sturgeon,[†] Misoo Ellison,[‡] Muriel T. Davisson,[§] and Katheleen J. Gardiner*[,†,∥,⊥]

[†]Department of Pediatrics, [‡]Colorado School of Public Health, [∥]Intellectual and Developmental Disabilities Research Center, and [⊥]Neuroscience, Human Medical Genetics, and Computational Biosciences Programs, University of Colorado Denver, Aurora, Colorado, United States

[§]The Jackson Laboratory, Bar Harbor, Maine, United States

Supporting Information

ABSTRACT: The Ts65Dn mouse model of Down syndrome (DS) is trisomic for orthologs of 88 of 161 classical protein coding genes present on human chromosome 21 (HSA21). Ts65Dn mice display learning and memory impairments and neuroanatomical, electrophysiological, and cellular abnormalities that are relevant to phenotypic features seen in DS; however, little is known about the molecular perturbations underlying the abnormalities. Here we have used reverse phase protein arrays to profile 64 proteins in the cortex, hippocampus, and cerebellum of Ts65Dn mice and littermate controls. Proteins were chosen to sample a variety of pathways and processes and include orthologs of HSA21 proteins and phosphorylation-dependent and -independent forms of non-HSA21 proteins. Protein profiles overall show remarkable stability to the effects of trisomy, with fewer than 30% of proteins altered in any brain region. However, phospho-proteins are less resistant to trisomy than their phospho-independent forms, and Ts65Dn display abnormalities in some key proteins. Importantly, we demonstrate that Ts65Dn mice have lost correlations seen in control mice among levels of functionally related proteins, including components of the MAP kinase pathway and subunits of the NMDA receptor. Loss of normal patterns of correlations may compromise molecular responses to stimulation and underlie deficits in learning and memory.

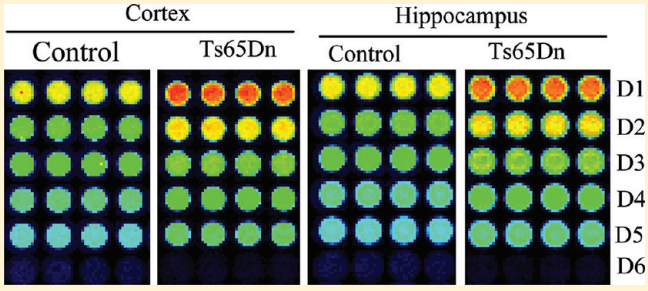

KEYWORDS: *Trisomy 21, protein profiles, MAP kinase, NMDA receptor, reverse phase protein array*

INTRODUCTION

Down syndrome (DS) is the most common genetic cause of intellectual disability (ID).[1] While ID in DS can be mild, the average IQ is 40−50.[2,3] With an incidence of one in approximately 750 live births, and as the average life span increases to beyond 50−60 years, there is an increasingly significant population requiring substantial support throughout life. Postnatal pharmacotherapies that could prevent or ameliorate some of the cognitive deficits would have important benefits for individuals with DS, their families, and society. DS is due to an extra copy of human chromosome 21 (HSA21). The increased expression level, due to dosage, of some subset of the trisomic genes is hypothesized to perturb normal regulation of cellular processes, resulting in the abnormalities in cell numbers, morphology, and sizes of the hippocampus and other brain regions that characterize the DS brain and likely underlie the cognitive deficits.

mRNA expression levels have been assayed in fetal brains, amniocytes, neurospheres and cell lines derived from DS, and in brain regions and other tissues and cells derived from some partial trisomy mouse models of DS (summarized in ref 4). In each of these systems, not all genes that are trisomic show elevated levels of transcription, many non-HSA21 genes show altered expression patterns, and there are clear model and tissue specificities in both sets of genes. It is difficult to predict the downstream consequences of these transcriptional deregulations, because mRNA levels are not robustly predictive of protein levels[5,6] and because most proteins are subject to post-translational modifications (PTMs) that regulate their levels of activity. Many responses to stimulation, including some tests of learning and memory, do not require immediate transcription, but rather depend initially on dynamic changes in PTMs and intracellular localization, for example, phosphorylation and sumoylation-driven shuttling between the cytosol and nucleus of the transcription factor ELK and learning in context fear conditioning.[7−9]

Recent reports of successes in rescuing learning and memory deficits in the Ts65Dn mouse model of DS suggest that postnatal pharmacotherapy for cognitive deficits in DS may be

Received: September 19, 2011
Published: January 3, 2012

   dx.doi.org/10.1021/pr2011582 | J. Proteome Res. 2012, 11, 1251−1263

practical. Drug treatments so far have been chosen to target DS-relevant cellular or neurophysiological abnormalities,[10−12] largely in the absence of knowledge about the underlying direct, and potentially indirect, HSA21 molecular causes.[12] An understanding of the molecular basis of abnormalities that underlie ID in DS may allow identification of new, possibly more specific and effective, targets for pharmacotherapies. There have been, however, few studies of protein levels in DS systems. Discovery-based studies using mass spectrometry have detected small numbers of abnormalities in whole brains minus cerebellum from the Ts65Dn partial trisomy mouse and in the embryonal stem cell line that is the parent of another DS partial trisomy mouse model, the Tc1,[13,14] but insightful interpretation is difficult when information on biological relationships among the proteins is lacking.[15] Hypothesis-driven studies using standard Western blot analysis have successfully identified abnormalities in brain regions of Ts65Dn in levels of a small number of HSA21 orthologous proteins and a few phosphoproteins.[13,16−18] In these and other DS systems, as with mRNA levels, trisomy does not necessarily result in increased expression at the protein level.

HSA21 encodes 550 gene models, of which only 161 are classical protein coding genes annotated in RefSeq and SwissProt databases and five are microRNAs.[19] Some functional information is available for most of these, but it must be considered incomplete. The remaining gene models include ∼150 that encode transcripts with open reading frames >50 amino acids and ∼250 that lack such orfs, and none of these has any functional annotation. Overexpression of even a subset of HSA21 genes at the mRNA and/or protein level is likely to increase their individual functional interactions and generate, in cascade reactions, complex perturbations in the activities of many non-HSA21 proteins and the pathways in which they function. Here, the sensitive and moderate throughput technique of Reverse phase Protein Arrays (RPA)[20−24] has been used to profile levels of 64 proteins in brains of the Ts65Dn mouse model of DS that is trisomic for orthologs of 88 HSA21 protein coding genes. Proteins measured include 12 with orthologs encoded by HSA21 and phosphorylation dependent and independent forms of signaling pathway components and receptors.

MATERIALS AND METHODS

Mice

The Ts65Dn mice[25] are maintained by mating trisomic females to C57BL/6JEi × C3H/HeSnJ (B6EiC3Sn) F1 hybrid males. Male mice, 6 controls and 5 trisomic, aged 4.4−7.8 months, were bred at The Jackson Laboratory (Bar Harbor, ME). Colonies were maintained in a room with HEPA-filtered air and a 14:10 light/dark cycle, fed a 6% fat diet and acidified (pH 2.5−3.0) water *ad libitum*. Littermates (Table 1) were housed in the same cage. All procedures were approved by The Jackson Laboratory's Institutional Animal Care and Use Committee and performed in accordance with National Institutes of Health guidelines for the care and use of animals in research. Ts65Dn mice were genotyped by quantitative (real time) polymerase chain reaction (qPCR) for genes in the trisomic segment.[26]

Tissue Processing and Preparation of Protein Lysates

Mice were sacrificed by cervical dislocation. The brain was removed and the cerebellum separated. Cerebellum and brain minus cerebellum were snap frozen in liquid nitrogen and stored at −80 °C until use. To optimally preserve protein profiles, including phosphorylation, prior to lysate preparation, tissues were heat stabilized in the Stabilizor T1 (Denator, AB) as described[27] following the manufacturer's directions. Briefly, tissues were removed from 80 °C and, without thawing, immediately placed in the sample cassette and inserted into the Stabilizor T1 where they were exposed to rapid heating to 95 °C under vacuum. This process has been shown to prevent normal post mortem proteolytic events and alterations in post translational modification.[27,28] After stabilization, brains minus cerebellum were dissected into hippocampus and cortex. Cortex, hippocampus and cerebellum tissue samples were weighed and whole tissue lysates were placed in 10 volumes of IEF buffer (8 M urea, 4% CHAPS, 50 mM Tris) and homogenized by sonication (three bursts of 5 s duration in Branson Sonic Power Co, Danbury, CT), followed by brief centrifugation to remove debris. Protein concentrations, determined using the 660 nM Protein Assay kit (Pierce), were within the range of 9−11 mg/mL for all samples. Information for each mouse on age, littermates, and weights of individual brain regions is provided in Table 1.

Table 1. Information for Individual Mice[a]

			tissue weight (mg)		
mouse	littermates	age	CR	HP	CB
C1	T1	7.8	108	26	68
C2	T2	7.7	97	35	60
C3	C4,C5	4.4	109	31	65
C4	C3,C5	4.4	117	26	74
C5	C3,C4	4.4	125	34	57
C6	T3	4.4	124	37	71
T1	C1	7.8	118	31	56
T2	C2	7.7	103	21	47
T3	C6	4.4	100	30	65
T4	T5	4.4	115	35	64
T5	T4	4.4	96	32	59

[a]Six controls (C1−C6) and five trisomic (T1−T5) were used in these experiments. Littermates were housed together. Age at sacrifice (months) and weights of each brain region (mg) are shown. CR, cortex; HP, hippocampus; CB, cerebellum.

Western Blots

Twenty micrograms of protein lysates per lane were separated at 170 V, constant voltage for 2.5 h on SDS-PAGE gels (8 or 10% depending upon size the proteins to be detected). Following electrophoresis, proteins were transferred to PVDF membranes at 250 mA constant current for 1.5 h. Membranes were blocked with 5% (w/v) Bovine Serum Albumin (BSA) in TBST (Tris-buffered saline, 0.1% Tween 20), followed by overnight incubation at 4 °C with primary antibody. Detection of bound primary antibodies was performed with alkaline-phosphatase-conjugated goat antirabbit (Invitrogen, Carlsbad, CA) or goat antimouse (Cell Signaling Technology, Danvers, MA) secondary antibodies. Signals were detected with CDP-Star Chemiluminescence reagent; imaging and quantitation were carried out using the Diana III CCD camera and Aida software (Raytest, Inc., Germany). All membranes were stripped in 0.2 M Glycine pH 2.5/0.05% Tween 20, at 70 °C for 20 min, and reprobed with actin antibody (Sigma, St. Louis, MO).

TIAM1 Isoforms

Inspection of spliced ESTs and curated mRNAs aligned with the human and mouse TIAM1 genes in the University of

dx.doi.org/10.1021/pr2011582 | J. Proteome Res. 2012, 11, 1251−1263

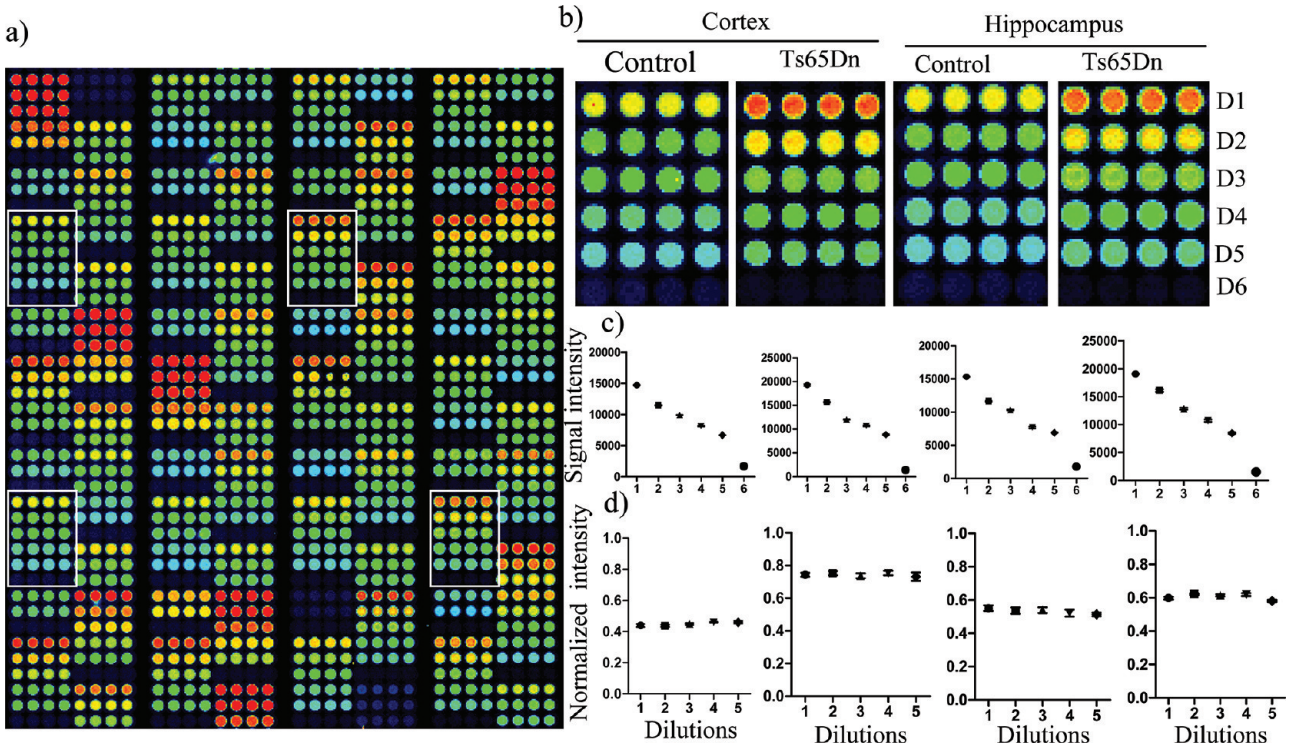

Figure 1. Representative RPA slide and data analysis. (a) Representative portion of a slide screened with an antibody to the HSA21 ortholog ITSN1, showing four replicates of a five point dilution series plus a blank spotted for each sample. (b) Enlargement of four sections in (a) illustrating the genotype differences in signal intensities. (c) Signal intensities of samples in (b) plotted vs dilution factor. (d) Signal intensities in (b) normalized to signals from SyproRuby staining of a separate slide, plotted vs dilution factor.

California Santa Cruz (UCSC) Genome Browser (http://genome.ucsc.edu) identified potential splice variants: (human) BC143970, BC143980, AI168629 and BE502041, and (mouse) BC065126, AK034803, AK136956 and NM_0011458. Partial transcript variants were assembled with the corresponding RefSeq mRNA sequences. Corresponding amino acid sequences were used to predict the molecular weight of each human and mouse isoform and identify TIAM1-specific bands detected by Western analysis.

Antibodies and Validation for RPA

Antibodies used in this study are listed in Supplementary Table S1 with supplier and dilution factor (Supporting Information). Reverse phase Protein Arrays (RPA) require highly specific antibodies.[20,24] Prior to use in RPA, each lot of each antibody was tested on Western blots of mouse brain lysates and verified to produce clean band(s) of the correct size(s) in the absence of significant background and nonspecific bands, that is, to produce predominant band(s) of explainable size. With the exception of TIAM1, that identifies bands in addition to those explained by alternative splicing and proteolytic cleavage, all antibodies listed in Table S1 are suitable for RPA. Supplementary Figure S1 shows a representative Western blot for five antibodies (Supporting Information).

Array Assembly and Printing

For each sample, lysates, neat plus four serial dilutions (dilution factor 0.8) and one buffer control were pipetted into V-shaped ABgene 384- well plates (Thermo Fisher Scientific, Rockford, IL). Samples were printed in quadruplicate onto nitrocellulose-coated glass slides (Grace Bio-Laboratories, Inc., Bend, OR) using an Aushon BioSystems 2470 Arrayer (Aushon BioSystems, Billerica, MA) with 185 μm pins and a single touch. All arrays were produced in a single print run. Slides were stored at 4 °C until use.

Antibody Detection and Array Staining

Slides were incubated in blocking solution (3% BSA (Sigma, St. Louis, MO) in TBST (Tris-buffered saline, 0.1% Tween 20)) for 4 h, followed by overnight incubation at 4 °C with primary antibody (antibody dilutions are provided in Table S1, Supporting Information). Detection of bound primary antibodies was performed by incubation for 90 min at room temperature with Fluorescence Alexa Fluor 555 goat antimouse or anti rabbit or rabbit antigoat (Invitrogen, Carlsbad, CA) secondary antibodies (1:2000). Slides were washed with TBST 3 times for 5 min and dried for 20 min at 30 °C. All the steps including and following the incubation with secondary antibody were performed in the dark. For normalization purposes, total protein in each spot was determined by staining three non sequential slides with SyproRuby reagent (Invitrogen) following the manufacturer's protocol.

Slide Scanning, Image Analysis, Quantification, Normalization and Review of Data Quality

Antibody hybridized slides and SyproRuby stained slides were scanned on a GenePix 4000B array slide scanner (Axon Instruments, Union City, CA) using GenePix Pro 4.0 software. Slide images were saved as TIFF files and the intensity of each spot quantified using the ScanArray Express software (PerkinElmer Inc., Waltham, MA). Images for each slide were manually inspected and those with excessive background or nonuniform signal intensities were discarded. Individual spot signal intensity was summarized as the median value subtracted from the adjacent background signal. For visual evaluation of the quality of RPA data, scatterplot graphs of antibody signal

dx.doi.org/10.1021/pr2011582 | J. Proteome Res. 2012, 11, 1251–1263

Table 2. Protein Levels in Ts65Dn Relative to Controls[a]

protein	CR	HP	CB	unchanged
Hsa21 proteins				
APP	39%***	20%**	18%**	
TIAM1_200	54%*	nc	ND	
TIAM1_150	41%#	nc	ND	
TIAM1_75	48%*	nc	ND	
TIAM1_70	48%*	nc	ND	
SOD1	44%**	37%*	nc	CCT8, CHAF1B, PRMT2
ITSN1	47%***	20%*	22%**	
DYRK1A	58%***	31%*	24%*	
DONSON	9%*	nc	−13%*	
ETS2	nc	nc	−9%*	
ADARB1	nc	15%#	15%*	
TRPM2	nc	nc	−9%#	
Signaling proteins, phosphorylation dependent forms				
pMEK1/2 (Ser 217/221)	nc	−14%*	−13%*	
pERK1/2(Tyr204)	47%*	nc	nc	
pELK1(Ser383)	38% **	nc	nc	
pRSK(Ser380)	25%##	nc	nc	pBRAF(Thr401), pCREB(Ser133), pJNK(Thr183/Tyr185), pCAMKIIA/B(Thr286),
pAKT(Ser473)	nc	nc	−15%*	pPKCA/B(Thr638/641)
pGSK3B(Ser9)	nc	nc	−19%**	
pPKCG(Thr514)	25%**	nc	38%**	
pMTOR (Ser2448)	nc	−10%#	nc	
pP70S6(Thr389)	nc	nc	20%*	
Signaling proteins, phosphorylation independent forms				
BRAF	37%***	nc	16%*	
CREB	nc	nc	−17%*	
AKT	13%*	nc	nc	
GSK3B	27%**	nc	nc	ERK1/2, PKCA, RSK, JNK, MTOR, MEK1/2
CAMKII	nc	nc	−9%*	
P35/25	nc	−11%*	nc	
CDK5	nc	−15%#	nc	
Apoptosis related proteins				
BAD	nc	nc	−10%*	
BCL2	nc	−12%*	−13%*	BAX, CASP3
pCASP9(Ser196)	10%*	nc	nc	
Receptors				
pGluR2(Tyr876)	nc	nc	−12%*	TRKA, BDNF, NR1, pNR1(Ser889), NR2A, pNR2A(Tyr1246), NR2B, pNR2B(Tyr1336), GluR3, GluR4
Miscellaneous				
pNUMB(Ser276)	12%*	nc	−12%*	
GFAP	9%*	nc	−11%*	
pGJA1(Ser368)	12%*	nc	nc	NUMB, GAD2, CTNNB1
SHH	10%*	nc	−8%*	
SYP	nc	−18%*	nc	
CAT	10%*	nc	nc	

[a]Values were calculated using 3-level mixed effects model and are relative to 100% in control mice. All data are from RPA, with the exception of TIAM1 which was analyzed by Western blots. CR, cortex; HP, hippocampus; CB, cerebellum. CTNNB1, β-catenin, component of the adherens junction; GAD2, glutamate decarboyxlase 2, GABA synthesis; GJA1, connexin 43, component of gap junctions; SYP, synaptophysin, synaptic vesicle membrane protein. Significant differences: *, $p < 0.05$; ** $p < 0.01$;*** $p < 0.001$. (##, $p < 0.05$ by the Student's t-test). #, differences approaching significance, $0.05 < p < 0.07$.

intensity, SyproRuby signal intensity, and signal intensity ratios (antibody to SyproRuby) vs the five point dilution series for all sample replicates were generated in PDF files using R software. Antibody and SyproRuby signal intensity curves are expected to be close to a dilution curve with slope = −0.8, while the signal intensity ratios are expected to be consistent for the five points of the dilution series. Examples are shown in Figure 1c and d. For quantitative evaluation of array data, EXCEL files for

dx.doi.org/10.1021/pr2011582 | J. Proteome Res. 2012, 11, 1251−1263

Table 3. RPA Reproducibility[a]

protein	exp #	C1	C2	C3	C4	C5	C6	T1	T2	T3	T4	T5
ITSN1	1	111	76	97	111	94	113	159	116	157	173	127
	2	104	92	92	100	94	112	152	120	142	166	124
GSK3B	1	115	85	96	100	89	114	134	103	131	153	112
	2	111	86	94	103	92	109	128	102	122	136	109
pERK1/2	1	135	64	107	111	89	89	171	89	143	193	129
	2	128	92	96	104	96	92	168	92	124	192	124

[a]Two slides each (Exp 1 and 2) were screened with the HSA21 protein ITSN1 and the non-HSA21 proteins, GSK3B and pERK1/2. C1−C6, control mice 1−6. T1−T5, Ts65Dn mice 1−5. For each mouse in each experiment, the values shown are the % of the mean normalized signal from control mice for that experiment.

dilutions and replicates were generated using the JAVA JXL package. Using the ScanArray signal intensity data, the EXCEL files display the ratios of antibody signal intensities to SyproRuby signal intensities for the 20 spots (4 replicates of 5 dilutions) of each sample, organized by sample type and sample ID. For each sample, the mean of the 20 ratios is calculated and, for visual evaluation of data quality, color coding is used to indicate spots with ratios within ±7.5%, ±7.5−10% and ±10−12.5% of the mean. Of 63 antibodies, 58 had more than 14 of 20 spots, for all samples, with signals that fell within 10% of the mean and the remaining five antibodies had at least 11 of 20. These were minimum criteria for inclusion of a slide in further analysis.

Statistical Analysis

After exclusion of technical outliers, each SyproRuby-normalized protein value was included in the statistical analyses if the level was within its mean ±3 standard deviations. This process eliminated on average <1% of the total observed data for each protein. Mean differences between genotypes (trisomy vs control, reported as % of control) were assessed using a three-level mixed effects model to account for the possible correlations among replicates and dilution levels within each mouse. To carry out a correlation analysis, data were reduced (i.e., one observation per mouse) using a mixed-effects model with different mice being the random effects. Protein values for each brain region of each individual of each genotype were used to compute Spearman correlation coefficients. Correlation coefficients greater than 0.8 were inspected graphically and a three-level mixed effect model was employed to determine the significance of the correlation slopes. All data analyses were carried out using SAS version 9.2 (SAS Institute Inc., Cary, NC). A two-tailed p-value <0.05 was considered statistically significant.

Graphical Display of Correlation Data

Spearman correlation data were organized in Excel files generated using the JAVA JXL package. For comparison of a given protein between genotypes (Ts65Dn vs control), the table displays all proteins that are either directly or inversely correlated with it in both genotypes (common correlations), and all proteins that are correlated with it in either control or Ts65Dn (genotype-specific correlations). Supplemental Table S3 shows all significant correlations ($r > 0.8$; $p < 0.05$) for all three brain regions. Correlation networks were created using JAVA JUNG2 software.

RESULTS

Protein Profiling in Mouse Brain

The goal of the protein measurements was to assess potential perturbations in pathways known to be relevant to learning/memory and other neurological abnormalities seen in DS or the Ts65Dn mice or postulated to underlie aspects of the DS neurological phenotype. The technique of RPA was chosen for this analysis because it provides the throughput required for measurement of a relatively large number (64) of proteins in a relatively large number (33) of samples (derived from cortex, hippocampus and cerebellum, from 5 trisomic Ts65Dn and 6 control mice). The required number of such measurements, with replicates, would not be practical by quantitative Western blots. RPA is also a technique that is sensitive and conservative of sample, requiring as little as 50 ug of lysate to spot ∼100 slides with replicate dilution series.[20−24] This feature is particularly important for analysis of more limited tissues, such as hippocampus. Proteins chosen for analysis included orthologs of some HSA21 proteins that are trisomic in the Ts65Dn and some, the majority, non-HSA21 orthologs that are components of signaling pathways such as MAP kinase and mTOR, subunits of the NMDA receptor, or involved in nerve growth factor signaling or apoptotic responses. These pathways and complexes were chosen because they are known or predicted to be abnormal in DS or in DS mouse models. Because RPA requires highly specific antibodies, many that are suitable for standard Western analysis cannot be used in RPA. Additional antibodies raised against human protein sequences do not cross react with mouse brain lysates with sufficient specificity. As a result, measurement of some proteins of interest was not possible. Proteins that were measured are listed in Table 2. Information on antibody source and dilutions is provided in Supplementary Table S1 (Supporting Information).

RPA has not previously been reported using mouse brain tissue nor for assaying perturbations resulting from multigene expression increases caused by trisomy. Initial experiments, therefore, involved validation of RPA technical and analysis protocols. Figure 1a shows a portion of a representative RPA slide spotted with whole cell lysates from cortex, hippocampus and cerebellum from Ts65Dn mice and controls, and screened with an antibody to the trisomic HSA21 ortholog ITSN1. The subarray enlargement (Figure 1b) clearly shows the qualitative effect on signal intensity of the five point sample dilution series, the similarities in signals among the four replicates, and the differences in signals between trisomic and control samples. Figure 1c shows results of one step in the standard quality control analysis where, for each sample set of 24 spots, antibody signal intensities are plotted vs dilution factor. This should produce a straight line with slope of −0.8. Signals from SyproRuby plotted vs dilution factor should also produce a straight line with slope of −0.8 (data not shown). Lastly, when antibody signals are normalized to corresponding SyproRuby signals, a plot of the ratio for all replicates and dilutions of a

dx.doi.org/10.1021/pr2011582 | J. Proteome Res. 2012, 11, 1251−1263

sample should produce a straight line with slope of zero, as shown in Figure 1d. Visual inspection of such plots provides a qualitative assessment of the reliability and reproducibility of the data.

Reproducibility of array quantitation was demonstrated by results of screening replicate slides with antibodies to pERK1/2, GSK3B and ITSN1. While sample signal intensities with the same antibody can vary between slides screened on different days due to technical issues, relative values of corresponding samples should be consistent. Table 3 shows the values of 11 samples (6 controls and 5 Ts65Dn) calculated as the percentage of the mean value of the 6 controls for the replicate slides. Relative values are highly reproducible. Supplementary Table S2 provides coefficients of variation (%CV) for controls and Ts65Dn samples for the three replicate slide pairs (Supporting Information). As a second validation, RPA results for selected antibodies were compared to values obtained by Western blots. Figure 2a shows results for DYRK1A and

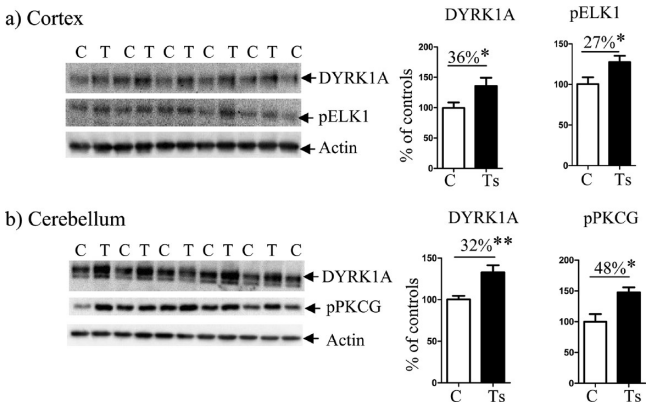

Figure 2. Western analysis for RPA validation. (a) DYRK1A and pELK1 measured in cortex. (b) DYRK1A and PKCG measured in cerebellum. C, control; T, Ts65Dn. Bar graphs represent quantitation of replicate Western blots; values are calculated relative to 100% for controls. White bars (C), control; black bars (Ts), Ts65Dn. *, $p < 0.05$; **, $p < 0.01$.

pELK1 in cortex, where increases of 36 and 27% ($p < 0.05$), respectively, in the Ts65Dn with respect to controls were measured; these compare with 58% ($p < 0.001$) and 38% ($p < 0.01$) obtained by RPA (Table 2). Figure 2b shows that, in cerebellum, increases in DYRK1A and pPKCG were 32% ($p < 0.01$) and 48% ($p < 0.05$), respectively, in Ts65Dn with respect to controls by Western analysis, vs 24% ($p < 0.05$) and 38% ($p < 0.01$) obtained by RPA (Table 2). Thus, abnormalities in Ts65Dn mice detected by RPA are replicated in direction and general percentage difference by Western analysis.

In total, RPA was used to measure levels of 11 HSA21 orthologous proteins (one additional HSA21 protein was measured by quantitative Western blots) and 52 non-HSA21 proteins. A subset of the latter included pairs of antibodies directed at phosphorylation dependent and phosphorylation independent forms of the same proteins.

HSA21 Protein Profiles

Results with 12 HSA21 proteins are summarized in Table 2. Trisomic samples showed increased levels of APP, ITSN1 and DYRK1A in all three brain regions, although increases are not always the 50% expected from gene dosage. The level of SOD1 was not elevated in cerebellum. Two trisomic HSA21 orthologs, the chaperone protein, CCT8, and the chromatin assembly factor, CHAF1B, showed no increases, and two, C21orf 60 (aka DONSON) and the transcription factor and oncogene, ETS2, showed modest decreases but only in cerebellum. The guanine nucleotide exchange factor, TIAM1, was investigated in cortex and hippocampus by Western analysis because the antibody was not suitable for RPA. Three alternatively spliced transcripts for mouse TIAM1 are annotated in the GenBank RefSeq protein database and two additional splice variants are predicted from inspection of human mRNAs in the UCSC Genome Browser (described in Methods). Together, these predict proteins of 622−1591 amino acids, with molecular weights of 70, 147, 159, 198, and 205 kDa. In addition, TIAM1 is proteolytically cleaved by caspase-3 to a 75 kDa form.[29] Thus, multiple bands are expected on Western blots, as seen in Figure 3. We quantitated four bands, the ~200 kD band that is likely a doublet of the 198 plus 205 kD bands, the 150 kD band that is likely a doublet of the 147 plus 155 kD bands and bands at ~75 and 70 kDa. Cortex, but not hippocampus, showed elevated levels of TIAM1 for the largest 200 kDa, the smallest 70 kD isoform and the 75 kDa proteolytic product (the increase in the 150 kDa band was close to significant ($p = 0.06$)). Orthologs of two HSA21 proteins, the protein arginine-methyltransferase, PRMT2 and the transient receptor potential cation channel, TRPM2, mapping to mouse chromosome 10 and not trisomic in the Ts65Dn mice, showed no significant increases relative to controls, although the pre-mRNA adenosine deaminase, ADARB1, also mapping to mouse chromosome 10 showed modest increases in both hippocampus and cerebellum.

Non-HSA21 Protein Profiles

Of the 52 non-HSA21 proteins, 26 showed altered levels in one or more brains regions. Cortex, hippocampus and cerebellum showed altered levels, respectively, of only 13, 6, and 14 of 52 proteins, indicating that protein levels overall are relatively stable to the effects of trisomy. Both increases and decreases are seen, with increases dominating in cortex (all 14 alterations) while decreases, 6 of 6 and 11 of 14, are more common in hippocampus and cerebellum. When levels of both phosphorylation dependent and phosphorylation independent forms of the same protein were measured, phosphorylation levels were more often altered, for example, 7 of 15 phosphorylation dependent forms compared with only 5 of 15 of the corresponding phosphorylation independent forms. The largest perturbations are 47 and 38% for pERK1/2 and pELK1 in cortex, and 38% pPKCG in cerebellum. Several abnormalities are modest (<20%); however, the sensitivity and the large number of replicate measurements in RPA allows accurate detection of small differences not quantifiable by Western analysis.

Among the components of the MAP kinase pathway, perturbations are not consistent among adjacent kinases in the cascade. For example, in cortex, pERK1/2 is elevated, but the upstream pMEK1/2 is not, and downstream pRSK and pELK1 are elevated, but pCREB is not. In hippocampus, perturbations to MAP kinase components are quite different; only pMEK1/2 is decreased. These observations are of particular interest for interpreting the molecular basis of deficits in hippocampal-dependent learning and memory seen in the Ts65Dn, and the potential contributions of altered MAP kinase signaling. Other region specific abnormalities include

dx.doi.org/10.1021/pr2011582 | J. Proteome Res. 2012, 11, 1251−1263

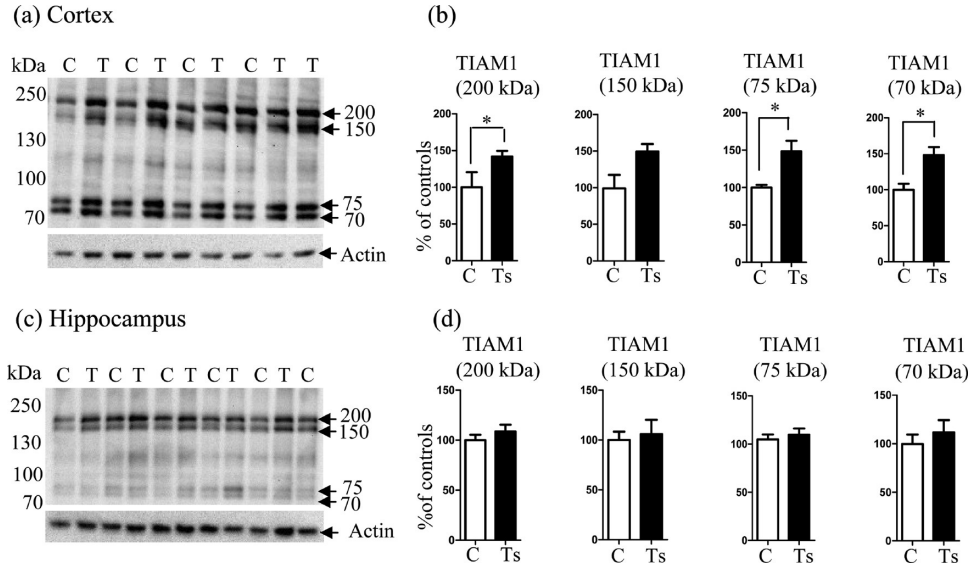

Figure 3. Western analysis of TIAM1. (a) Cortex; (c) Hippocampus; arrows indicate protein isoforms as discussed in the text. C, control; T, Ts65Dn. (b and d) Bar graphs represent quantitation of replicate Western blots; values are calculated relative to 100% for controls. White bars (C), control; black bars (Ts), Ts65Dn. *, $p < 0.05$.

decreases in pGSK3B in cerebellum, an increase in GSK3B in cortex, and several changes in apoptosis related proteins.

In spite of increased levels of APP and TIAM1 that directly interact with NMDA receptors[30−33] and ITSN1 that indirectly interacts with them,[34] no perturbations in phosphorylated or phosphorylation independent forms of the NR1, NR2A or NR2B subunits were detected. Increased levels of phosphorylated NUMB, a protein involved in regulation of cell number during neurogenesis,[35] however, were detected in cortex, possibly related to elevated levels of APP and ITSN1,[34,36,37] although decreases were detected in cerebellum.

Correlation among Proteins

The Ts65Dn mice are not maintained on an inbred background and individuals will have a combination of 0, 1, or 2 alleles from C3H and C57BL6/J, in addition to the DBA allele in the extra Chromosome 16 segment.[25] Previous work has shown variability in protein and phosphorylation levels among individuals in a group of Ts65Dn mice and littermate controls,[16] and indeed patterns in such variability were used to predict variability in locomotor response to treatment with the NMDA receptor antagonist, MK-801.[38]

Figure 4a shows the levels in hippocampus of three proteins in individual mice. In control mice, DYRK1A values range from 0.16 to 0.25, pERK1/2 from 0.20 to 0.33 and ITSN1 from 0.30 to 0.42, while in Ts65Dn, the values of the same proteins range from 0.21 to 0.31, 0.23 to 0.43 and 0.43 to 0.51, respectively. Thus, among both control and trisomic mice, the level of a specific protein varies by ~25% to as much as 50%-100%. This variability overlaps with the average increases in trisomic proteins seen in the Ts65Dn mice. We also note the appearance of patterns in the interindividual variability. In controls, mice C2 and C6 have the lowest values for all three proteins and C1 and C4, the highest values. In the Ts65Dn, mice T2 and T4 have the lowest and highest values, respectively, for DYRK1A and pERK1/2, but with ITSN1 there appears little similarity to the patterns with the other proteins and indeed there is much less variability among the five Ts65Dn mice. Figure 5a shows a similar analysis of the levels in cortex of the HSA21 ortholog APP and the NMDA

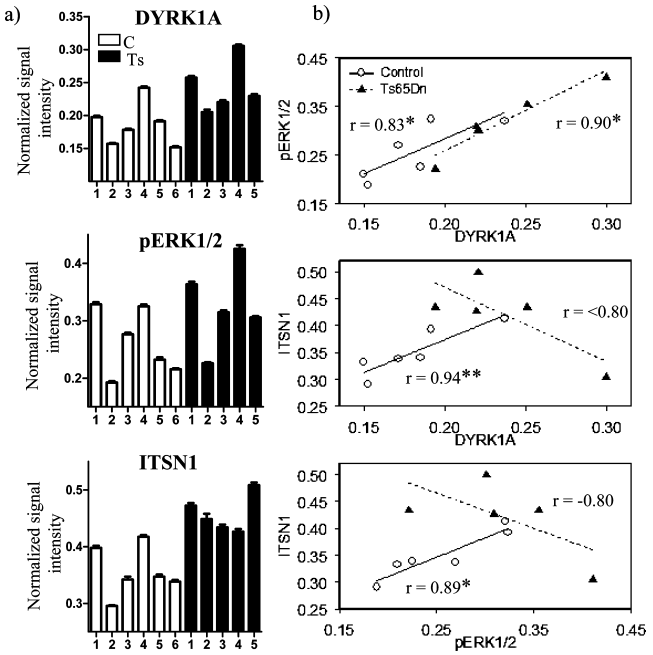

Figure 4. Correlations between DYRK1A, ITSN1 and pERK1/2 in hippocampus. (a) Relative signal intensities (normalized to SyproRuby signals) of antibodies to the indicated proteins in hippocampus from individual mice. White bars, control mice #s1−6; black bars, Ts65Dn mice #1−5. DYRK1A and ITSN1 are HSA21 encoded proteins.(b) Scatter plots of pairwise comparisons of levels of proteins in a). r, Spearman correlation coefficient. ○, control mice; ▲, Ts65Dn mice. *, $p < 0.05$; **, $p < 0.005$; #, $p < 0.0001$. For $r < 0.8$, correlations were considered not significant.

receptor subunits NR2B and NR1. These patterns do not reflect either age or relationships between littermates (Table 1). Based on observations of these types of patterns, we investigated correlations between all pairs of proteins in each genotype in each brain region. We retained as significant all correlations with $r > 0.8$ (Spearman correlation analysis; Supplementary Table S2, Supporting Information). Figures 4b

dx.doi.org/10.1021/pr2011582 | J. Proteome Res. 2012, 11, 1251−1263

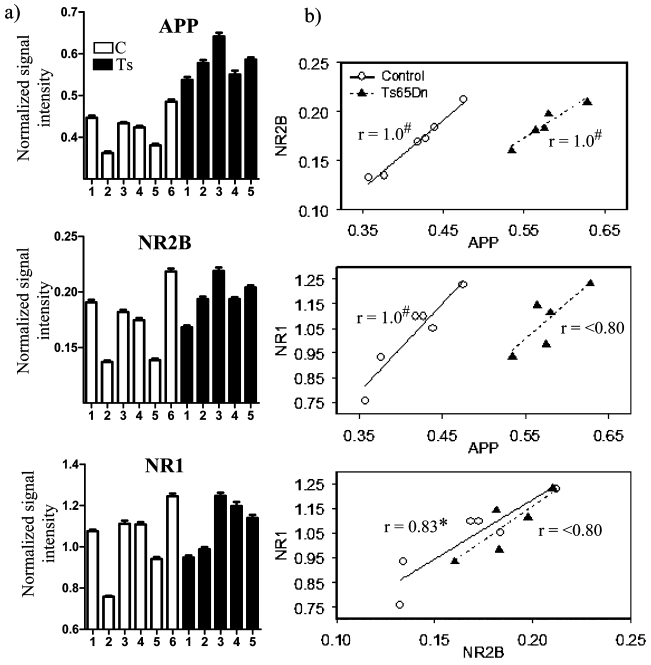

Figure 5. Correlations between APP and subunits NR2B and NR1 of the NMDA receptor in cortex. (a) Relative signal intensities (normalized to SyproRuby signals) of antibodies to the indicated proteins from individual mice. White bars, control mice #s1−6; black bars, Ts65Dn mice #1−5. APP is an HSA21 encoded protein. (b) Scatter plots of pairwise comparisons of levels of proteins in a). r, Spearman correlation coefficient. ○, control mice; ▲, Ts65Dn mice. *, $p < 0.05$; **, $p < 0.005$; #, $p < 0.0001$.

and 5b show scatter plots of levels in individual mice of the pairs of proteins analyzed in Figures 4a and 5a. Correlations with $r > 0.8$ ($p < 0.05$) are consistent with the similarities in patterns seen in the bar graphs in Figures 4a and 5a, whereas those with $r < 0.8$ show greater scatter, have higher p values, and are consistent with the lack of similarities in bar graph patterns.

We retrieved from Supplementary Table S2 those correlations involving proteins with known functional associations within the MAP kinase signaling pathway. We found, in addition to many non-HSA21 proteins, some HSA21 proteins. Scatter plots for each correlation of interest were inspected and those with higher p values ($p > 0.05$) were excluded. In Figure 6, networks of proteins from the MAP kinase cascade with significant correlations and p values <0.05 are shown. Notable in Figure 6a are several correlations in hippocampus in control mice, e.g. between pERK1/2 and pELK1, and between ERK1/2 and pERK1/2, that are absent in the Ts65Dn mice. Indeed, there are few correlations common to controls and Ts65Dn. Correlations between pERK-DYRK1A and BRAF-DYRK1A are preserved, but of the correlations seen in controls with the HSA21 protein ITSN1 (which is overexpressed in Ts65Dn), all are absent in Ts65Dn mice. In cortex (Figure 6b), most correlations seen in controls are preserved in the Ts65Dn, but there are also many Ts65Dn-specfic correlations. We next reviewed correlations involving subunits of the NMDA receptor. Figure 7 shows networks of NMDA receptor subunits with similarly significant correlations. Again in hippocampus (Figure 7a), most correlations seen in controls are lost in the Ts65Dn. In addition, both hippocampus and cortex (Figure 7b) show losses of correlations in the Ts65Dn between the HSA21

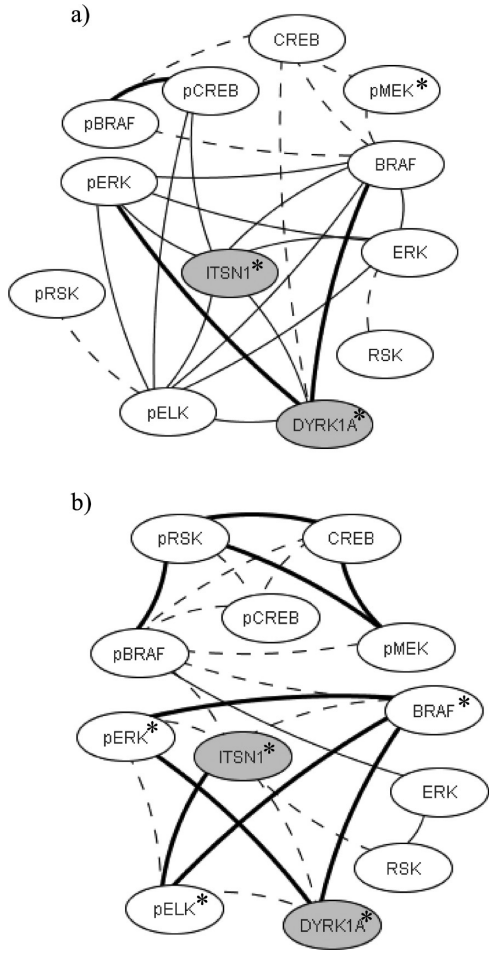

Figure 6. Correlations among HSA21 proteins ITSN1 and DYRK1A and components of the MAP kinase signaling cascade in (a) hippocampus and (b) cortex. Correlations between protein levels were determined as in Figure 4; only correlations with $r > 0.8$, with linear scatter plots and $p < 0.05$ were considered significant and are included. Heavy solid lines, correlations seen in controls and Ts65Dn; thin solid lines, correlations seen only in controls; dashed lines, correlations seen only in Ts65Dn. Gray circles, HSA21 proteins; open circles, non-HSA21 proteins. Phosphorylation dependent and independent forms are shown separately. Correlations do not require altered levels in Ts65Dn with respect to controls. *, protein levels were significantly different between Ts65Dn and controls.

protein APP (which is overexpressed) and NMDA receptor subunits. We have previously shown a failure of dynamic responses in MAP kinase signaling in Ts65Dn stimulated with the NMDA receptor antagonist, MK-801.[16] We suggest that losses in correlated levels of component proteins may contribute to such failed responses to stimuli, and may also similarly underlie impaired or slowed learning responses that also require MAP kinase signaling.

We reviewed the correlations in Table S2 for additional functional relationships (Supporting Information). Figure 8 shows that normal correlations seen in hippocampus of control mice between HSA21 proteins ITSN1 and APP and NUMB, which is relevant to cell number and dendritic spine morphology, are lost in Ts65Dn hippocampus (Figure 8a), and that HSA21 protein correlations with apoptosis related proteins seen in cortex of controls are also lost in Ts65Dn mice (Figure 8b).

dx.doi.org/10.1021/pr2011582 | J. Proteome Res. 2012, 11, 1251−1263

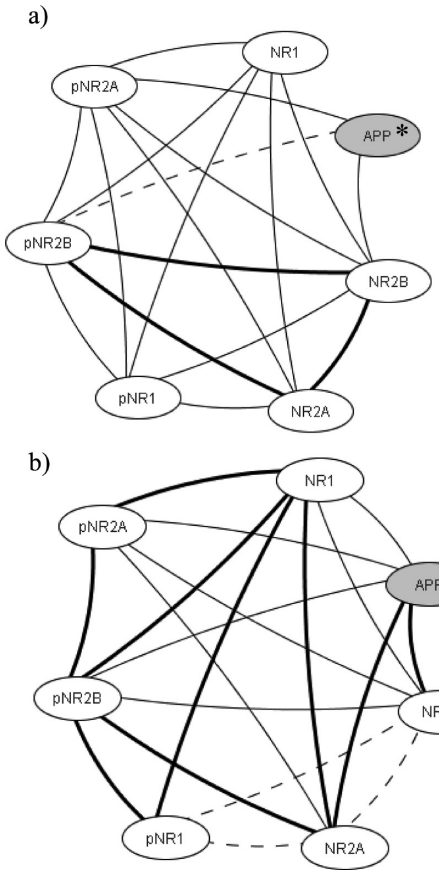

Figure 7. Correlations among levels of the HSA21 protein APP and NMDA receptor subunits in (a) hippocampus and (b) cortex. Correlations between protein levels were determined as in Figure 5; only correlations with $r > 0.8$, with linear scatter plots and $p < 0.05$ are shown. Heavy solid lines, correlations seen in controls and Ts65Dn; thin solid lines, correlations seen only in controls; dashed lines, correlations seen only in Ts65Dn. Gray circles, HSA21 proteins; open circles, non-HSA21 proteins. Phosphorylation dependent and independent forms are shown separately. Correlations do not require altered levels in Ts65Dn with respect to controls. *, protein levels were significantly different between Ts65Dn and controls.

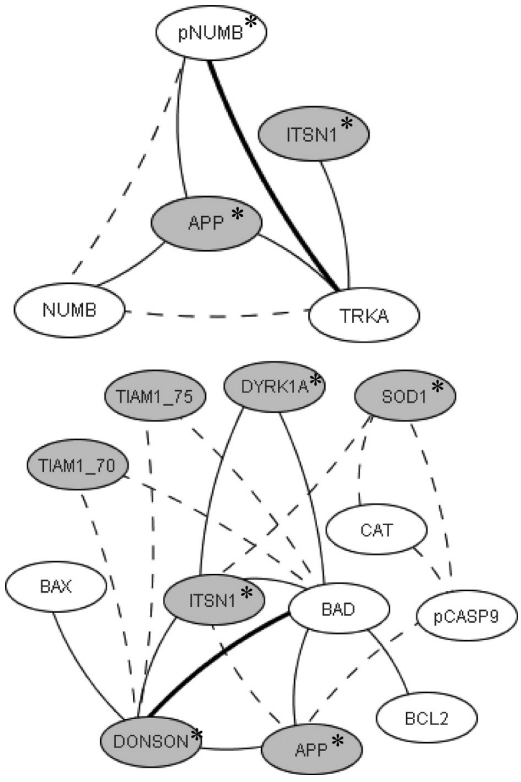

Figure 8. Correlations among HSA21 proteins and (a) NUMB in cortex, (b) apoptosis pathway components in hippocampus. Only correlations with $r > 0.8$, with linear scatter plots and $p < 0.05$ are shown. Heavy solid lines, correlations seen in controls and Ts65Dn; thin solid lines, correlations seen only in controls; dashed lines, correlations seen only in Ts65Dn. Gray circles, HSA21 proteins; open circles, non-HSA21 proteins. *, protein levels were significantly different between controls and Ts65Dn.

DISCUSSION

The phenotype of DS is the result of a complex problem of multigene overexpression. In addition, we do not know which HSA21 genes are overexpressed and when and where, we do not know all the functions of all HSA21 genes, and what we do know about HSA21 genes indicates that their normal functions relate to many pathways of relevance to learning and memory.[39,40] To develop an understanding at the molecular level of how trisomy 21 results in deficits in learning and memory, a pathway approach is necessary. For DS studies, pathway analysis has the advantage that it allows interrogation of the integrated effects of all overexpressed HSA21 genes, without the necessity of understanding all the underlying individual gene contributions. Here we elected to assess pathway perturbations at the protein level. This accommodates potential effects of post-transcriptional regulation of trisomic gene expression and can more directly reflect the levels of protein activity by including phosphorylation levels. We selected proteins for measurement with the goal of sampling many pathways of known relevance to learning and memory and known or predicted perturbation in DS or DS mouse models.

Profiles in three brain regions of the Ts65Dn showed abnormalities in levels of fewer than half of all proteins assayed and therefore are relatively robust to trisomy of 88 classical protein coding genes. Importantly, not all trisomic genes are overexpressed at the protein level. Of nine proteins tested that are trisomic in the Ts65Dn, the three, APP, ITSN1 and DYRK1a, that were overexpressed in all three brain regions, together have substantial support for contributions to brain anomalies, learning and memory deficits and development of Alzheimer's disease in DS.[41−46] SOD1, that was overexpressed in cortex and hippocampus but not cerebellum, has frequently been implicated in oxidative stress in DS and mice over-expressing SOD1 display deficits in learning and memory.[47] TIAM1, that is overexpressed in cortex but not hippocampus, has not been investigated explicitly in DS or mouse models, but it has been shown to participate in regulation of neuronal cell polarity and overexpression in cultured hippocampal neurons results in abnormalities of dendritic spines.[33,48,49] It will be of interest to explore further the possible effects of overexpression of TIAM1 in cortex. Nothing is known with respect to DS about the chromatin assembly factor, CHAF1B, or the chaperone protein, CCT8, and nothing at all is known about the function of C21orf60 (aka DONSON). The transcription factor ETS2, which also was not overexpressed (and actually decreased in cerebellum), has been linked to oxidative stress

dx.doi.org/10.1021/pr2011582 | J. Proteome Res. 2012, 11, 1251−1263

and is postulated to contribute to the increased rate of apoptosis observed in cultured DS fetal neurons, where in contrast to adult mouse brain tissues, ETS2 is overexpressed.[50,51] Expression levels observed here of trisomic proteins, elevated or not, may not reflect expression at other times. Indeed, protein levels of APP and SOD1 and mRNA levels of DYRK1A were not elevated in brains of five month old Ts65Dn mice.[52] The failure to observe increased expression at one time point does not allow exclusion of genes as candidates for contributing to the development of the DS phenotype. More comprehensive analysis with additional ages, including developmental time points, is required.

It is unarguably of interest to understand how expression of trisomic genes is regulated in DS and how, in some cases, overexpression is repressed at the transcriptional and/or translational level. Alternatively, however, for a focus on development of pharmacotherapies for cognitive deficits in DS, it is the downstream consequences of altered HSA21 gene expression that are of the greatest significance, because it is among these that targets for successful drug treatments are more likely to be found. The current work has focused, therefore, on measurement of non-HSA21 proteins involved in several signaling pathways and cellular complexes. The resulting data in Table 2 are complex and not amenable to simple interpretation. Perturbations differ among brain regions and do not present a simple picture within a pathway. For example, perturbations in phosphorylation are not consistent among consecutive steps in the classical MAP kinase cascade. However, a DS-centric interpretation emphasizes that the initial perturbation in the Ts65Dn mice (and DS) is not a complete blockade of one step, such as can be achieved in an in vitro cell system using a MEK inhibitor,[53] or in a mouse model by a single gene mutation.[54] Rather, it is due to the modest overexpression of many HSA21 genes, genes that influence many pathways and where there is also cross talk among pathways.[39,40] Table 2 likely contains three categories of abnormalities: (i) those caused by elevated expression of one or more HSA21 orthologs and in turn causing or contributing to a DS neurological phenotypic feature; (ii) those caused by elevated expression of one or more HSA21 orthologs but irrelevant to or benign with respect to any neurological phenotype; and (iii) those that are compensatory responses to abnormalities in (i) or (ii). It is the abnormalities in (i) that are necessary to control in order to ameliorate the neurological phenotype. Conversely, normalizing those in (iii) is likely to further exacerbate the phenotype. It is unfortunate that it is not obvious from the studies here which proteins belong to which category. However, further inspection of the protein profiles has shown that, rather than determination of simple average differences between genotypes as provided in Table 2, it is interindividual variations in the patterns of protein levels that provides insight. The networks in Figures 4−8 show that one consequence of trisomy is the loss of correlations among the levels of functionally related and neurologically important proteins. Notably, these losses can occur in the absence of average genotype differences in the levels of network components.

Interindividual variations in levels of protein expression can be caused by factors in addition to genotype. Similar environments were provided for all mice (light, temperature, nutrition, housing with littermates). Housing included instances of both same genotype and mixed genotype groups (Table 1). Weights of brain regions did not show any significant relationship to genotype or age, or to genotype of littermates (Table 1). Stress can affect protein levels, in particular of protein modifications. While mice were removed to a separate room immediately prior to sacrifice, the order of sacrifice of individuals in a single cage could affect levels of some protein modifications. Lastly, as noted above, Ts65Dn are not maintained on an inbred background, and allelic variation will exist. However, while multiple factors can contribute to individual variation in protein expression levels, it remains notable that correlations among some proteins show robust genotype specificities.

The losses of correlations among components of the MAP kinase pathway and the NMDA receptor complex can be used to interpret the molecular basis of several behavioral abnormalities and drug responses seen in the Ts65Dn mice. First, treatment with the NMDA receptor antagonist, MK-801, produces an abnormal behavioral response (exaggerated hyperactivity) in the Ts65Dn mice. The same treatment is associated with abnormal changes in phosphorylation patterns of signaling proteins in cortex and hippocampus.[16] Second, Ts65Dn mice are impaired in the hippocampal-based task context fear conditioning (CFC),[55] which is known to require dynamic responses in phosphorylation levels of MAP kinase pathway components, among them pERK1/2 and pELK1.[9] Third, the CFC learning impairment is rescued by treatment with the NMDA receptor antagonist, memantine.[55] Preliminary data suggest that memantine also rescues MAP kinase pathway correlations (manuscript in preparation). It is noteworthy that both MAP kinase and NMDAR correlations in control mice include the HSA21 orthologs, APP, ITSN1 and DYRK1A. Thus, we suggest that increased levels of HSA21 proteins result in losses of correlations among functionally associated components of the MAP kinase pathway and the NMDA receptor complex, and that these losses can occur with or without altered levels of specific components. Furthermore, we suggest that loss of normal patterns of correlations can compromise molecular responses to stimulation and underlie deficits in learning and memory. Such a hypothesis is not without precedence and is supported by recent proteome data from patients with Alzheimer's Disease.[56] It is important to note that detection of correlations in these and other pathways in controls, and their loss in the Ts65Dn, does not require knowledge of functional relationships with HSA21 proteins or, indeed, measurement of any HSA21 proteins.

Analysis of gene expression at the protein level, even with RPA, remains a relatively low throughput process when compared with measurements of tens of thousands of transcripts possible by microarrays. It is well established, however, that levels of mRNA do not correlate well with corresponding protein levels.[5,6] To examine this association for the interindividual variation in the Ts65Dn mice, we compared protein results obtained here with mRNA results reported by Sultan et al.[57] Data from cortex and cerebellum were available from both studies. Sultan et al[57] assigned trisomic genes to three groups: genes with consistently higher expression in Ts65Dn with respect to controls (i.e., elevated as expected from gene dosage in all trisomic individuals), genes with some overlap in expression levels between Ts65Dn and controls, and genes with complete overlap of expression levels in Ts65Dn and controls (i.e., compensated for gene dosage and unchanged in trisomy relative to controls). As shown in Table 4, there are similarities and differences between protein and mRNA expression in interindividual variability. For all individuals,

Table 4. Individual Variability in Protein and mRNA Levels of HSA21 Orthologs[a]

	protein		mRNA		
Protein	CX	CB	CX	CB	top 30
APP	↑	↑	↑	↑	+
CCT8	nc	nc	↑	↑	+
TIAM1	↑	nd	↑	nc	
SOD1	↑	nc	nd	nd	+
DONSON	↑ v	↓v	nd	nd	+
ITSN1	↑	↑	↑ v		
CHAF1B	nc	nc	nd	nd	
DYRK1A	↑	↑ v	nc	nc	+
ETS2	nc	↓v	↑	nc	+
TRPM2	nc	↓v	nd	nd	
ADARB1	nc	↑ v	nd	nd	
PRMT2	nc	nc	nd	nd	

[a]Genes were divided into three groups as in Sultan et al.:[57] genes with trisomic levels that did not overlap with control levels (arrows, increase or decrease); those with trisomic levels that partially overlapped with controls (v, variable); and those with levels indistinguishable from controls (nc, no change). nd, not determined. +, among the top 30 genes most often found increased in DS or DS mouse models.[4]

APP and TIAM1 expression was elevated and distinguishable from controls at both the protein and mRNA levels. For ITSN1, while protein levels were elevated with respect to controls in both regions and trisomic mRNA levels were elevated in cerebellum, mRNA levels partially overlapped with controls in cortex. For CCT8, protein expression was indistinguishable from controls in both brain regions, but mRNA levels were elevated in both regions. Differences with ETS2 were complicated: trisomic protein levels in cortex were indistinguishable from controls and partially overlapping with controls in cerebellum, while mRNA levels were elevated in cortex and indistinguishable from controls in cerebellum. Lastly, DYRK1A, one of the most intensively studied HSA21 genes, was elevated at the protein level in cortex and variably elevated in cerebellum, but not elevated at the mRNA level. These comparisons indicate that expression of trisomic genes is governed, not only by complex and gene-specific mechanisms operating at the transcriptional, translational and/or post-translational levels, but also by individual, possibly stochastic, genomic background, and/or subtle environmental, influences affecting both mRNA and protein levels. As a last comparison, Table 4 indicates the six genes that were also found among the 30 genes most often increased in expression in DS and DS mouse model studies.[4] A discussion of differences and similarities of expression perturbations in non-HSA21 genes is beyond the scope of the current work and will be provided elsewhere.

As a last point, technical issues will affect protein profiles and complicate developing a broad understanding of molecular abnormalities in the Ts65Dn and other DS model systems. Differences obviously will occur when, instead of whole cell lysates from specific brain regions, as examined here and in Siarey et al,[17] whole brain minus cerebellum[13] or subcellular fractions of specific brain regions[16] are examined. In particular, abnormalities detected in a single subcellular fraction, nuclear, cytosolic or membrane, or with opposite directions of change in two fractions, may be undetectable in whole lysates. An additional point is that the large number of replicates possible using RPA (e.g., 15−20) provides sensitivity for small changes that is often not possible using Western blot analysis. Thus, while there are many similarities, especially in general characteristics of phosphorylation abnormalities, between the current work and that reported in Siddiqui,[16] there are also differences. Other differences may arise from differences in the age of the mice examined,[18] as discussed.[16] Notably, when 12 month old Ts65Dn were examined, patterns of abnormalities in apoptosis-related proteins that differed from those noted in Table 2 were found.[58] Either brain region or age may have contributed to observations that APP, SOD1 and DYRK1A were not overexpressed in Ts65Dn,[52] in contrast to observations here. Less well recognized is that protein profiles will be affected by the protocol for protein lysate preparation, which can have significant consequences for levels of phosphorylation in particular. A recent report demonstrated that, without the inclusion of phosphatase inhibitors, phosphatase activity continued during tissue handling and lysate preparation, and resulted in substrate and site-specific changes in phosphorylation levels with time and temperature.[59] This is a particular concern during subcellular fractionation, especially for synaptosome preparations because of the extra time (several hours) involved.[13] Use of kinase inhibitors alone may produce an inaccurate picture in Ts65Dn relative to controls, in part because the activity of a prominent protein phosphatase, calcineurin, is perturbed in the Ts65Dn due to overexpression of its HSA21-encoded inhibitor, RCAN1 (aka DSCR1).[46] For lysate preparation here, we used heat stabilization, which inactivates all enzymes, both kinases and phosphatases, and produces significant differences in protein profiles when compared even to standard snap frozen lysate preparations.[27,28] Lastly, pooling of samples from different individuals, as in,[13] while practical for mass spectrometry procedures, will obscure subtleties of interindividual variation. To develop a reliable picture of protein and pathway perturbations, one goal in protein profiling, therefore, must be to develop a standard consistent method of lysate preparation.

SUMMARY

We have identified brain region-specific abnormalities in both trisomic HSA21 orthologs and non-HSA21 phosphorylated and nonphosphorylated forms of pathway components. Measuring the levels of a large number (64) of proteins allowed us to identify networks of correlated proteins representing four pathways/processes, MAP kinase signaling, NMDA receptors, NUMB protein interactions, and the apoptosis pathway. In each network, levels of one or more HSA21 proteins are correlated with non-HSA21 proteins in brains of control mice. In Ts65Dn mice, where the levels of these HSA21 proteins are elevated, correlations are lost between HSA21 and non-HSA21 proteins, and among non-HSA21 proteins. Elevated levels of APP, ITSN1 and DYRK1A may make major contributions to the perturbed correlations, or more likely, they represent only a few of the total contributions. Other HSA21 encoded proteins also influence post translational modification; among them are kinases, a protein methyltransferase and components of the ubiquitin and sumoylation pathways, each a reasonable candidate for contributing to alterations in levels or activities of non-HSA21 proteins.[39,40] Lastly, measurements here represent basal levels of proteins, reflecting a relatively unstimulated (home cage) molecular state. While a valid starting point, the ability of protein levels to modulate in

dx.doi.org/10.1021/pr2011582 | J. Proteome Res. 2012, 11, 1251−1263

response to stimulation is both unpredictable (as yet) and more important. Undoubtedly, if additional proteins were measured, a more complete picture of trisomy perturbations would emerge, adding details to pathways annotated here and possibly identifying additional losses of correlated protein levels. Future efforts will characterize changes in patterns of correlations in the Ts65Dn mice in response to drug treatments; this should help to identify critical abnormalities and potentially more specific drug targets.

■ ASSOCIATED CONTENT

Supporting Information

Supplementary tables and figures. This material is available free of charge via the Internet at http://pubs.acs.org.

■ AUTHOR INFORMATION

Corresponding Author

*E-mail: katheleen.gardiner@ucdenver.edu. Tel: 303-724-0572. Fax: 303-724-3838.

■ ACKNOWLEDGMENTS

This work was supported by the National Institutes of Health HD065235, the Crnic Institute for Down Syndrome and the Fondation Jerome Lejeune. Mice raised at The Jackson Laboratory were funded by National Institutes of Health NICHD contract HD73265.

■ REFERENCES

(1) CDC, Centers for Disease Control and Prevention. Improved National Prevalence for 18 Major Birth Defects. *Morbidity Mortal. Wkly. Rep.* **2006**, *54*, 6−12.

(2) Chapman, R. S.; Hesketh, L. J. Behavioral phenotype of individuals with Down syndrome. *Ment. Retard. Dev. Disabil. Res. Rev.* **2000**, *6*, 84−95.

(3) Silverman, W. Down syndrome: cognitive phenotype. *Ment. Retard. Dev. Disabil. Res. Rev.* **2007**, *13*, 228−36.

(4) Vilardell, M.; Rasche, A.; Thormann, A.; Maschke-Dutz, E.; Pérez-Jurado, L. A.; Lehrach, H.; Herwig, R. Meta-analysis of heterogeneous Down Syndrome data reveals consistent genome-wide dosage effects related to neurological processes. *BMC Genomics* **2011**, *12*, 229.

(5) Maier, T.; Güell, M.; Serrano, L. Correlation of mRNA and protein in complex biological samples. *FEBS Lett.* **2009**, *583*, 3966−73.

(6) Schwanhäusser, B.; Busse, D.; Li, N.; Dittmar, G.; Schuchhardt, J.; Wolf, J.; Chen, W.; Selbach, M. Global quantification of mammalian gene expression control. *Nature* **2011**, *473*, 337−42.

(7) Yang, S. H.; Jaffray, E.; Hay, R. T.; Sharrocks, A. D. Dynamic interplay of the SUMO and ERK pathways in regulating Elk-1 transcriptional activity. *Mol. Cell* **2003**, *12*, 63−74.

(8) Salinas, S.; Briançon-Marjollet, A.; Bossis, G.; Lopez, M. A.; Piechaczyk, M.; Jariel-Encontre, I.; Debant, A.; Hipskind, R. A. SUMOylation regulates nucleo-cytoplasmic shuttling of Elk-1. *J. Cell Biol.* **2004**, *165*, 767−73.

(9) Sananbenesi, F.; Fischer, A.; Schrick, C.; Spiess, J.; Radulovic, J. Phosphorylation of hippocampal Erk-1/2, Elk-1, and p90-Rsk-1 during contextual fear conditioning: interactions between Erk-1/2 and Elk-1. *Mol. Cell. Neurosci.* **2002**, *21* (3), 463−76.

(10) Braudeau, J.; Delatour, B.; Duchon, A.; Lopes-Pereira, P.; Dauphinot, L.; de Chaumont, F.; Olivo- Marin, J. C.; Dodd, R. H.; Hérault, Y.; Potier, M. C. Specific targeting of the GABA-A receptor {alpha}5 subtype by a selective inverse agonist restores cognitive deficits in Down syndrome mice. *J. Psychopharmacol.* **2011**, *25* (8), 1030−1042.

(11) Faizi, M.; Bader, P. L.; Tun, C.; Encarnacion, A.; Kleschevnikov, A.; Belichenko, P.; Saw, N.; Priestley, M.; Tsien, R. W.; Mobley, W. C.; Shamloo, M. Comprehensive behavioral phenotyping of Ts65Dn mouse model of Down Syndrome: Activation of β(1)-adrenergic receptor by xamoterol as a potential cognitive enhancer. *Neurobiol. Dis.* **2011**, *43*, 397−413.

(12) Gardiner, K. J. Molecular basis of pharmacotherapies for cognition in Down syndrome. *Trends Pharmacol. Sci.* **2010**, *31*, 66−73.

(13) Fernandez, F.; Trinidad, J. C.; Blank, M.; Feng, D. D.; Burlingame, A. L.; Garner, C. C. Normal protein composition of synapses in Ts65Dn mice: a mouse model of Down syndrome. *J. Neurochem.* **2009**, *110*, 157−69.

(14) Wang, Y.; Mulligan, C.; Denyer, G.; Delom, F.; Dagna-Bricarelli, F.; Tybulewicz, V. L.; Fisher, E. M.; Griffiths, W. J.; Nizetic, D.; Groet, J. Quantitative proteomics characterization of a mouse embryonic stem cell model of Down syndrome. *Mol. Cell. Proteomics* **2009**, *8* (4), 585−95.

(15) Sun, Y.; Dierssen, M.; Toran, N.; Pollak, D. D.; Chen, W. Q.; Lubec, G. A gel-based proteomic method reveals several protein pathway abnormalities in fetal Down syndrome brain. *J. Proteomics* **2011**, *74*, 547−57.

(16) Siddiqui, A.; Lacroix, T.; Stasko, M. R.; Scott-McKean, J. J.; Costa, A. C.; Gardiner, K. J. Molecular responses of the Ts65Dn and Ts1Cje mouse models of Down syndrome to MK-801. *Genes Brain Behav.* **2008**, *7*, 810−80.

(17) Siarey, R. J.; Kline-Burgess, A.; Cho, M.; Balbo, A.; Best, T. K.; Harashima, C.; Klann, E.; Galdzicki, Z. Altered signaling pathways underlying abnormal hippocampal synaptic plasticity in the Ts65Dn mouse model of Down syndrome. *J. Neurochem.* **2006**, *98*, 1266−77.

(18) Gardiner, K.; Davisson, M. T.; Crnic, L. S. Building protein interaction maps for Down syndrome. *Briefings Funct. Genomics Proteomics* **2004**, *3*, 142−56.

(19) Sturgeon, X.; Gardiner, K. J. Transcript catalogs of human chromosome 21 and orthologous chimpanzee and mouse regions. *Mamm. Genome* **2011**, *22*, 261−71.

(20) Espina, V.; Mehta, A. I.; Winters, M. E.; Calvert, V.; Wulfkuhle, J.; Petricoin, E. F. 3rd; Liotta, L. Protein microarrays: molecular profiling technologies for clinical specimens. *Proteomics* **2003**, *3* (11), 2091−100.

(21) Nishizuka, S.; Charboneau, L.; Young, L.; Major, S.; Reinhold, W. C.; Waltham, M.; Kouros-Mehr, H.; Bussey, K. J.; Lee, J. K.; Espina, V.; Munson, P. J.; Petricoin, E. F. 3rd.; Liotta, L. A.; Weinstein, J. N. Proteomic profiling of the NCI-60 cancer cell lines using new high-density reverse-phase lysate microarrays. *Proc. Natl. Acad. Sci. U.S.A.* **2003**, *100* (24), 14229−34.

(22) Wulfkuhle, J. D.; Edmiston, K. H.; Liotta, L. A.; Petricoin, E. F. 3rd. Technology insight: pharmacoproteomics for cancer--promises of patient-tailored medicine using protein microarrays. *Nat. Clin. Pract. Oncol.* **2006**, *3* (5), 256−68.

(23) Espina, V.; Wulfkuhle, J.; Calvert, V. S.; Liotta, L. A.; Petricoin, E. F. 3rd. Reverse phase protein microarrays for theranostics and patient-tailored therapy. *Methods Mol. Biol.* **2008**, *441*, 113−28.

(24) Voshol, H.; Ehrat, M.; Traenkle, J.; Bertrand, E.; van Oostrum, J. Antibody-based proteomics: analysis of signaling networks using reverse protein arrays. *FEBS J.* **2009**, *276* (23), 6871−9.

(25) Davisson, M. T.; Schmidt, C.; Reeves, R. H.; Irving, N. G.; Akeson, E. C.; Harris, B. S.; Bronson, R. T. Segmental trisomy as a mouse model for Down syndrome. *Prog. Clin. Biol. Res.* **1993**, *384*, 117−33.

(26) Liu, D. P.; Schmidt, C.; Billings, T.; Davisson, M. T. Quantitative PCR genotyping assay for the Ts65Dn mouse model of Down syndrome. *Biotechniques* **2003**, *35*, 1170−4 , 1176, 1178.

(27) Svensson, M.; Boren, M.; Sköld, K.; Fälth, M.; Sjögren, B.; Andersson, M.; Svenningsson, P.; Andren, P. E. Heat stabilization of the tissue proteome: a new technology for improved proteomics. *J. Proteome Res.* **2009**, *8*, 974−81.

(28) Ahmed, M. M.; Gardiner, K. J. Preserving protein profiles in tissue samples: differing outcomes with and without heat stabilization. *J. Neurosci. Methods* **2011**, *196* (1), 99−106.

(29) Qi, H.; Juo, P.; Masuda-Robens, J.; Caloca, M. J.; Zhou, H.; Stone, N.; Kazanietz, M. G.; Chou, M. M. Caspase-mediated cleavage

of the TIAM1 guanine nucleotide exchange factor during apoptosis. *Cell Growth Differ.* **2001**, *12*, 603−11.
(30) Cousins, S. L.; Hoey, S. E.; Anne Stephenson, F.; Perkinton, M. S. Amyloid precursor protein 695 associates with assembled NR2A- and NR2B-containing NMDA receptors to result in the enhancement of their cell surface delivery. *J. Neurochem.* **2009**, *111*, 1501−13.
(31) Hoe, H. S.; Fu, Z.; Makarova, A.; Lee, J. Y.; Lu, C.; Feng, L.; Pajoohesh-Ganji, A.; Matsuoka, Y.; Hyman, B. T.; Ehlers, M. D.; Vicini, S.; Pak, D. T.; Rebeck, G. W. The effects of amyloid precursor protein on postsynaptic composition and activity. *J. Biol. Chem.* **2009**, *284*, 8495−506.
(32) Tolias, K. F.; Bikoff, J. B.; Burette, A.; Paradis, S.; Harrar, D.; Tavazoie, S.; Weinberg, R. J.; Greenberg, M. E. The Rac1-GEF Tiam1 couples the NMDA receptor to the activity-dependent development of dendritic arbors and spines. *Neuron* **2005**, *45*, 525−38.
(33) Tolias, K. F.; Bikoff, J. B.; Kane, C. G.; Tolias, C. S.; Hu, L.; Greenberg, M. E. The Rac1 guanine nucleotide exchange factor Tiam1 mediates EphB receptor-dependent dendritic spine development. *Proc. Natl. Acad. Sci. U.S.A.* **2007**, *104*, 7265−70.
(34) Nishimura, T.; Yamaguchi, T.; Tokunaga, A.; Hara, A.; Hamaguchi, T.; Kato, K.; Iwamatsu, A.; Okano, H.; Kaibuchi, K. Role of numb in dendritic spine development with a Cdc42 GEF intersectin and EphB2. *Mol. Biol. Cell* **2006**, *17*, 1273−85.
(35) Johnson, J. E. Numb and Numblike control cell number during vertebrate neurogenesis. *Trends Neurosci.* **2003**, *26* (8), 395−6.
(36) Kyriazis, G. A.; Wei, Z.; Vandermey, M.; Jo, D. G.; Xin, O.; Mattson, M. P.; Chan, S. L. Numb endocytic adapter proteins regulate the transport and processing of the amyloid precursor protein in an isoform-dependent manner: implications for Alzheimer disease pathogenesis. *J. Biol. Chem.* **2008**, *283*, 25492−502.
(37) Roncarati, R.; Sestan, N.; Scheinfeld, M. H.; Berechid, B. E.; Lopez, P. A.; Meucci, O.; McGlade, J. C.; Rakic, P.; D'Adamio, L. The gamma-secretase-generated intracellular domain of beta-amyloid precursor protein binds Numb and inhibits Notch signaling. *Proc. Natl. Acad. Sci. U.S.A.* **2002**, *99*, 7102−7.
(38) Nguyen, C. D.; Costa, A. C.; Cios, K. J.; Gardiner, K. J. Machine learning methods predict locomotor response to MK-801 in mouse models of down syndrome. *J. Neurogenet.* **2011**, *25*, 40−51.
(39) Gardiner, K.; Costa, A. C. The proteins of human chromosome 21. *Am. J. Med. Genet., Part C* **2006**, *142C*, 196−205.
(40) Sturgeon, X.; Ahmed, M. M.; Li, T.; Gardiner, K. J. Pathways to cognitive deficits in Down syndrome. *Prog. Brain Res.* **2012**, in press.
(41) Trazzi, S.; Mitrugno, V. M.; Valli, E.; Fuchs, C.; Rizzi, S.; Guidi, S.; Perini, G.; Bartesaghi, R.; Ciani, E. APP-dependent up-regulation of Ptch1 underlies proliferation impairment of neural precursors in Down syndrome. *Hum. Mol. Genet.* **2011**, *20*, 1560−73.
(42) Nixon, R. A. Endosome function and dysfunction in Alzheimer's disease and other neurodegenerative diseases. *Neurobiol. Aging* **2005**, *26*, 373−82.
(43) Lott, I. T.; Head, E.; Doran, E.; Busciglio, J. Beta-amyloid, oxidative stress and down syndrome. *Curr. Alzheimer Res.* **2006**, *3*, 521−8.
(44) Tejedor, F. J.; Hämmerle, B. MNB/DYRK1A as a multiple regulator of neuronal development. *FEBS J.* **2011**, *278*, 223−35.
(45) Yabut, O.; Domogauer, J.; D'Arcangelo, G. Dyrk1A overexpression inhibits proliferation and induces premature neuronal differentiation of neural progenitor cells. *J. Neurosci.* **2010**, *30* (11), 4004−14.
(46) Keating, D. J.; Chen, C.; Pritchard, M. A. Alzheimer's disease and endocytic dysfunction: clues from the Down syndrome-related proteins, DSCR1 and ITSN1. *Ageing Res. Rev.* **2006**, *5*, 388−401.
(47) Harris-Cerruti, C.; Kamsler, A.; Kaplan, B.; Lamb, B.; Segal, M.; Groner, Y. Functional and morphological alterations in compound transgenic mice overexpressing Cu/Zn superoxide dismutase and amyloid precursor protein [correction]. *Eur. J. Neurosci.* **2004**, *19*, 1174−90.
(48) Zhang, H.; Macara, I. G. The polarity protein PAR-3 and TIAM1 cooperate in dendritic spine morphogenesis. *Nat. Cell Biol.* **2006**, *8*, 227−37.
(49) Shirazi Fard, S.; Kele, J.; Vilar, M.; Paratcha, G.; Ledda, F. (2010). Tiam1 as a signaling mediator of nerve growth factor-dependent neurite outgrowth. *PLoS One* **2010**, *5*, e9647.
(50) Sanij, E.; Hatzistavrou, T.; Hertzog, P.; Kola, I.; Wolvetang, E. J. Ets-2 is induced by oxidative stress and sensitizes cells to H(2)O(2)-induced apoptosis: implications for Down's syndrome. *Biochem. Biophys. Res. Commun.* **2001**, *287*, 1003−8.
(51) Wolvetang, E. J.; Bradfield, O. M.; Hatzistavrou, T.; Crack, P. J.; Busciglio, J.; Kola, I.; Hertzog, P. J. Overexpression of the chromosome 21 transcription factor Ets2 induces neuronal apoptosis. *Neurobiol. Dis.* **2003**, *14*, 349−56.
(52) Choi, J. H.; Berger, J. D.; Mazzella, M. J.; Morales-Corraliza, J.; Cataldo, A. M.; Nixon, R. A.; Ginsberg, S. D.; Levy, E.; Mathews, P. M. Age-dependent dysregulation of brain amyloid precursor protein in the Ts65Dn Down syndrome mouse model. *J. Neurochem.* **2009**, *110*, 1818−27.
(53) Gioeli, D.; Wunderlich, W.; Sebolt-Leopold, J.; Bekiranov, S.; Wulfkuhle, J. D.; Petricoin, E. F.; Conaway, M.; Weber, M. J. Compensatory pathways induced by MEK inhibition are effective drug targets for combination therapy against castration-resistant prostate cancer. *Mol. Cancer Ther.* **2011**, *10*, 1581−90.
(54) Wang, X.; Nadarajah, B.; Robinson, A. C.; McColl, B. W.; Jin, J. W.; Dajas-Bailador, F.; Boot-Handford, R. P.; Tournier, C. Targeted deletion of the mitogen-activated protein kinase kinase 4 gene in the nervous system causes severe brain developmental defects and premature death. *Mol. Cell. Biol.* **2007**, *27* (22), 7935−46.
(55) Costa, A. C.; Scott-Mckean, J. J.; Stasko, M. R. Acute injections of the NMDA receptor antagonist memantine rescue performance deficits of the Ts65Dn mouse model of Down syndrome on a Fear conditioning Test. *Neuropsychopharmacology* **2008**, *33* (7), 1624−32.
(56) Britschgi, M.; Rufibach, K.; Bauer-Huang, S. L.; Clark, C. M.; Kaye, J. A.; Li, G.; Peskind, E. R.; Quinn, J. F.; Galasko, D. R.; Wyss-Coray, T. Modeling of pathological traits in Alzheimer's disease based on systemic extracellular signaling proteome. *Mol. Cell. Proteomics* **2011**, *10*, M111.008862.
(57) Sultan, M; Piccini, I; Balzereit, D; Herwig, R; Saran, N. G; Lehrach, H; Reeves, R. H; Yaspo, M. L. Gene expression variation in Down's syndrome mice allows prioritization of candidate genes. *Genome Biol.* **2007**, *8* (5), R91.
(58) Rueda, N.; Flórez, J.; Martínez-Cué, C. The Ts65Dn mouse model of Down syndrome shows reduced expression of the Bcl-X(L) antiapoptotic protein in the hippocampus not accompanied by changes in molecular or cellular markers of cell death. *Int. J. Dev. Neurosci* **2011**, *29*, 711−6.
(59) Espina, V.; Mueller, C.; Edmiston, K.; Sciro, M.; Petricoin, E. F.; Liotta, L. A. Tissue is alive: New technologies are needed to address the problems of protein biomarker pre-analytical variability. *Proteomics Clin. Appl.* **2009**, *3*, 874−82.